

Friction Stir Welding of 6mm thick carbon steel underwater and in air.

P.Baillie, S.W. Campbell, A. M. Galloway, S. R. Cater, N.A. McPherson

Abstract—This study compared the mechanical and microstructural properties produced during friction stir welding (FSW) of S275 structural steel in air and underwater. Post weld tests assessed the tensile strength, micro-hardness, distortion, Charpy impact toughness and fatigue performance in each case. The study showed that there was no significant difference in the strength, hardness or fatigue life of the air and underwater specimens. However, Charpy impact toughness was shown to decrease for the underwater specimens and was attributed to the presence of a slightly less angular grain structure than the samples welded in air. Reduced angular and longitudinal distortion was observed in the underwater welded plate compared to the plate welded in air.

Keywords—Charpy impact toughness, distortion, fatigue, friction stir welding (FSW), micro-hardness, underwater.

INTRODUCTION

Friction Stir Welding (FSW) is a thermo-mechanical process in which two metals are joined together in the solid state, to produce a high integrity, high quality joint [1], [2]. Compared with conventional arc welding processes, there are a number of benefits including; low distortion, minimal chemical segregation, enhanced strength and no detrimental effects to hardness due to grain refinement in the stir zone [3]-[6].

Although the process has reached a stage of technical maturity for the “light alloys”, its application to metals such as steel, nickel and titanium has been slower to develop due to the severe loads and temperatures the tool experiences during the welding process [7], [8]. Tool design and the development of advanced materials for FSW of steel has therefore become a significant area of research in recent years, focusing specifically on improving tool lifespan [9]. This is the key to the future economic viability of the process. Perrett et al. [10] investigated friction stir welding of industrial steels using two different tool materials; polycrystalline boron nitride (pcBN) and a W-Re/pcBN composite. In both cases, welds in excess of 40m were completed without tool probe failure or any signs of weld defects. In addition to this Sorensen [11] studied the wear and fracture sensitivity of three grades of pcBN tools and obtained a tool life of approximately 60m when welding structural steel.

The welding parameters in FSW include; tool traverse speed, rotational speed, vertical force and traverse force. It has been reported that by varying these parameters, the microstructural and mechanical properties can be precisely controlled, allowing for a repeatable, fully-autonomous joining process which produces almost defect free welds [12]. Fujii et al. [13] studied the effect of welding speed using three types of carbon steel; interstitial free (IF) steel, S12C (0.12wt.%C) and S35C (0.34wt.%C). In each case, the strength of the joint increased with increasing welding speed, with the exception of the S35C steel which peaked at 200mm/min. Hardness was also measured as a function of welding speed and the following results were obtained; the IF steel showed no significant gain in hardness, the S12C steel showed a linear increase in hardness and the S35C steel peaked again at 200mm/min. The results were explained by considering the relationship between the peak temperature and the A_1 or A_3 point on the iron-carbon phase diagram. When FSW is performed in the ferrite-austenite two-phase region, the microstructure is refined and the highest strength is achieved. Lakshminarayanan et al. [14] also reported increases in strength and hardness during FSW of 409M ferritic stainless steel, where the coarse ferrite grains in the base material were converted to a very fine duplex structure consisting of ferrite and martensite.

To date, research into the subject of underwater FSW has been limited. Liu et al. [15] performed a study, which determined the effect of welding speed on the microstructures and mechanical properties produced when welding 2219 aluminium alloy underwater. The results showed a significant increase in the tensile strength of the underwater joint in comparison with arc welds in the same material, which was attributed to the increased cooling rate preventing the deterioration of strengthening precipitates. Given the increasing interest in FSW for subsea and shipbuilding applications, it is essential that further research be completed to assess the feasibility of underwater FSW for steels. Some limited work has been carried out on steel [16,17]. The work [16] on quench and tempered HY80 steel, although very limited, highlighted that the wet stir zone and TMAZ had smaller grains than the dry stir zone and the base material, there were no significant issues with micro hardness. The increases in micro hardness were 52% and 70% for the dry stir and the wet stir respectively.

The present study reports on the comparison between the mechanical and microstructural properties produced in S275

structural steel when friction stir welded in air and underwater.

EXPERIMENTAL

S275 hot rolled structural steel was used in this study and was supplied in the form of plates measuring 2000 x 200 x 6mm (length x width x thickness). The chemical composition of the plates was 0.12% carbon; 0.25% silicon; 0.84%Mn; 0.007% Sulphur; 0.017% phosphorus; 0.007% nitrogen and 0.032% aluminium. The yield and tensile strengths of the plate are 353N/mm² and 509N/mm² respectively, and the elongation was 32.4%.

The S275 steel plates were welded with no milling of their mating edges and no removal of the surface scale or primer. Double sided friction stir welds were created in both the air and underwater conditions using the hybrid WRe-pcBN, Q70 (70 vol.%cBN) friction stir welding tool shown in Fig. 1.

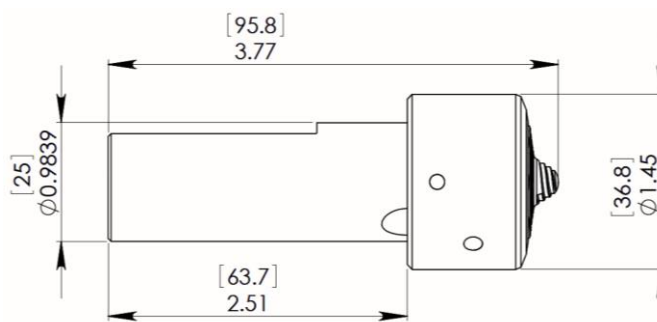


Fig. 1 Geometry of FSW tool

All welds were performed in the counter clockwise (CCW) direction by embedding the tool to a reference level of 4.8 mm below the surface from both sides, and a travel speed of 100 mm/min and rotational speeds as shown in Table 1. The effect of this is to create a material flow vertically downwards in the weld towards the backing bar. This process is used to eliminate root defects in the weld. The friction stir mode used was position control in both cases. The higher rotation speed in the underwater weld was an attempt to compensate for the enhanced cooling effect underwater. On the basis of the parameters used, this would class the weld as a ‘slow’ weld [18]. In the case of the air welds, an argon gas shield was also used to prevent the welding zone and tool from oxidizing. After welding there was no evidence of tool wear or oxidation from the underwater weld.

	Air FSW		Underwater FSW	
	Travel speed (mm/min)	Speed of rotation (revs/min)	Travel speed (mm/min)	Speed of rotation (revs/min)
Side 1	100	200	100	240
Side2	100	200	100	240

Table 1 Main welding parameters for each weld.

Post weld angular and longitudinal distortion was measured using an optical distance sensor control linked to a LabVIEW program that scanned the workpiece according to a pre-defined grid pattern. Each plate was secured on four locating points, which were calibrated using the optical distance sensor to result in zero deformation at these locations, spaced 380 x 800 mm apart. It was also assumed that the plates were initially flat prior to the welding process. Distortion measurements were recorded in 10 mm increments in both the longitudinal and transverse directions.

Transverse and longitudinal tensile tests, fabricated in accordance with BN EN ISO 4136: 2011, were performed to assess the strength of the welded joints (three in each direction for both air and underwater FSW). The tensile specimens were 6mm thick and 25mm wide in the test zone.

Charpy impact toughness was determined using BS EN ISO 148-1:2010. As the specimens were sub-size (5mm) all the initial results were scaled up to a 10x10mm equivalent using a factor of 1.5. The specimens (three for each location) were machined perpendicular to the weld centreline with notch positions -6, -4, -2, 0, +2, +4, +6 mm from the weld centre. The minus (-) notation is the retreating side and the plus (+) notation is the advancing side.

Micro-hardness was measured in accordance with BS EN ISO 6507-1: 2005 using a Mitutoyo MVK-G1 hardness tester. The load was 0.2kg for 15 secs.

RESULTS AND DISCUSSION

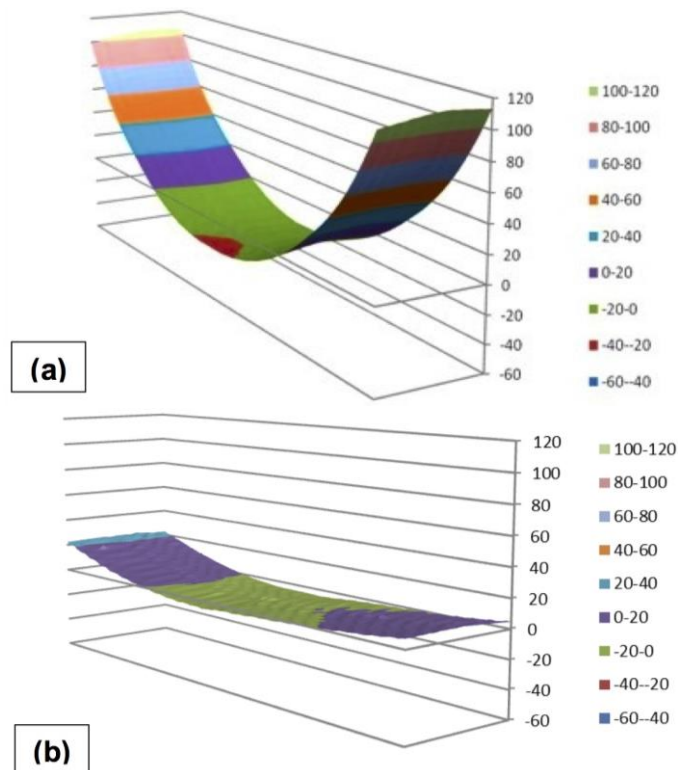
Distortion

The deformation profile for both the air and underwater FSW plates are shown in Fig. 2. A submerged arc welded (SAW) DH36 steel plate of the same dimension has been included to highlight the significant variation in distortion profile. All three plates show symmetrical distortion in the longitudinal direction. However, it is clear that the magnitude of distortion varies significantly between the FSW and the SAW plates. The underwater FSW plate exhibited the lowest distortion, with a deviation in the range of 5 to -1.5 mm from the zero reference-plane. The air FSW plate showed a slightly larger deviation in the range of 25 to -5mm, while the SAW plate showed the largest deviation in the range of 110 to -20mm.

This can be explained by considering the difference in heat input between each of the welds. The heat input calculated by McPherson et al. [19] for the arc welded plate is 3.79 KJ/mm. The heat input for the FSW plates was calculated using (1) and (2) where f_1 is the process efficiency [20].

$$Power = \frac{\left(2 \frac{rev}{min}\right) (Spindle Torque)}{60} \quad (1)$$

$$Heat Input = f_1 \left(\frac{Power}{Travel rate} \right) \quad (2)$$



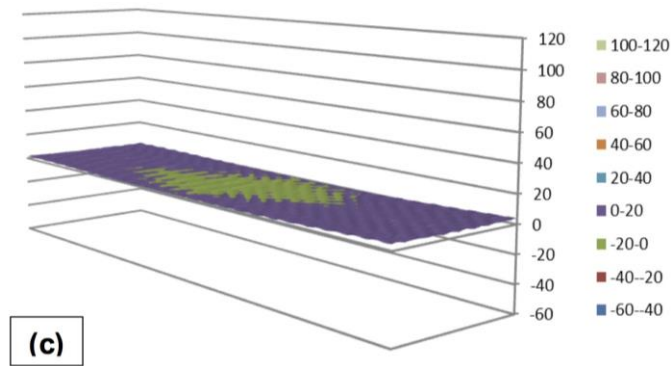


Fig. 2 Distortion profiles for (a) submerged arc welded DH36 steel, (b) air FSW plate, and (c) underwater FSW plate. Y-axis value indicates distortion from the zero-reference plane measured in mm

Heat input was calculated to be 3.01 and 4.29 KJ/mm for the air and underwater welded plates respectively. The additional heat input of 1.28 KJ/mm for the underwater plate was estimated to compensate for the high heat dissipation to the surrounding water, which in turn would reduce thermal stress in the parent plate and subsequently reducing distortion. This is equivalent to an increase in heat input of 42%.

The large variation between the distortion in the SAW and FSW plates could be attributed to two factors. Firstly, FSW plates are subjected to a higher degree of restraint during welding because of the clamping involved. This restraint mitigates against movement during welding and hence reduces distortion. The SAW process involves a phase change during welding as it goes from liquid to solid, whereas FSW is a solid-state process. This means that the magnitude of the thermal stresses will be larger for the SAW plate due to the volume changes (longitudinal and transverse shrinkage) experienced during solidification and subsequent cooling to room temperature. However there is also a phase change involved using this process

Macrostructure

The macro-etched images in Fig. 3(a) and (b) are the underwater and air welds respectively and they show full penetration welds from both sides with an overlap region of approximately 3.6 mm. The letters A and B represent the overlap region, and thermo mechanically affected zone (TMAZ) respectively. Table 2 describes the physical sizes of the two welds. Clearly the underwater weld is larger. It is not surprising the second side width of the underwater weld is larger due to the greater heat input used there. However, the first side weld width of the first side in the underwater weld is significantly wider (42%) than the air weld width. There could also be an issue related to tool condition which would affect the weld geometry. These welds were not produced under conditions of exactly the same tool condition.

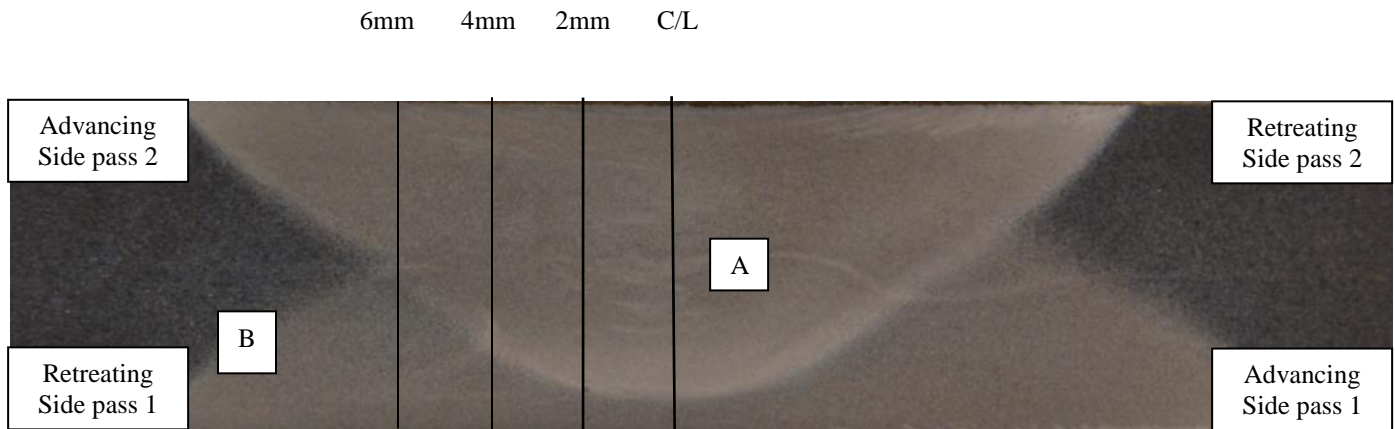


Figure 3(a) Underwater friction stir welded macro section showing the overlap region at A and the area of the TMAZ shown in Figure 5(a) is at B.

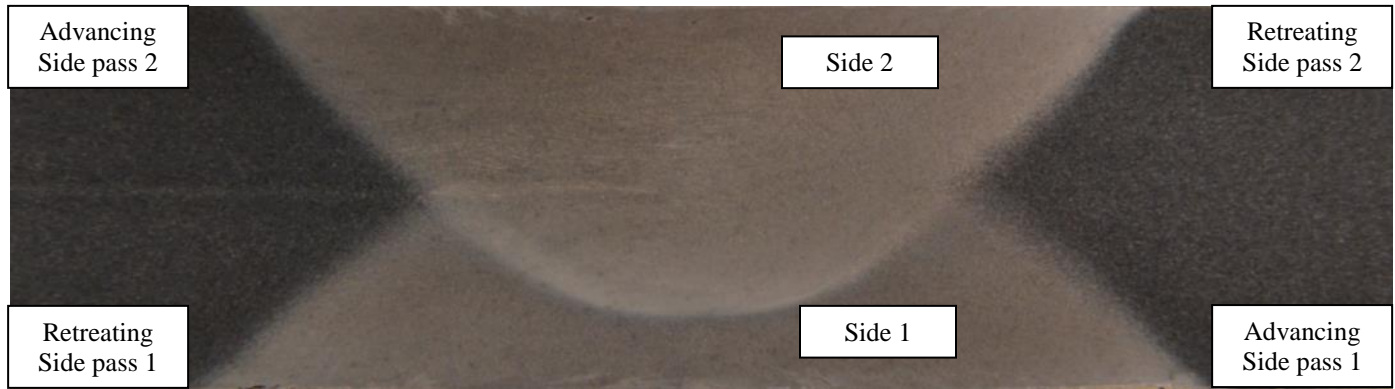


Figure 3(b) Air friction stir welded macro section showing less second side penetration than in the underwater sample shown in Figure 5(b)

	Air FSW (mm)	Underwater FSW (mm)	Increase (%)
Side 1 weld width	16.4	21.7	42.5
Side 2 weld width	14.5	17.8	22.7
Side 2 penetration	5	5.4	8.0

Table 2 Dimensions of the two welds

Microstructure

The microstructure of each zone was classified using an Olympus GX-51 microscope. The parent material shown in Fig. 4 has a microstructure of ferrite-pearlite with the effect of the lower carbon being obvious from the higher ferrite content. The parent plate had an average grain size of 13.5 micron. The structure shown is a cross section at right angles to the major rolling direction, whereas in the case of the underwater weld, the microstructure was seen as being banded and had been taken parallel to the rolling direction. The remnants of this can be seen in Figure 5(b). Within the TMAZ, Figs. 5 (a) and (b), it can be seen that the pearlite begins to degenerate in both cases, but to a greater extent, apparently, in the underwater treated sample. The average ferrite grain size is 11.4 micron which is marginally smaller than the parent plate grain size. The ferrite grains within the air FSW plate (Fig. 5 (b)) are smaller, but with a significant variation in size. The smaller recrystallised grains vary between 2.2 and 4 micron. However there are a number of grains around 12 micron, which is close to the parent plate size. In addition the TMAZ was narrow in both samples and as a result did not significantly contribute to the strength or toughness of the weld. The overlap regions, Figs. 6 (a) and (b), shows significant grain refinement as a result of severe plastic deformation (SPD) and recrystallization. The relative grain sizes are 3.8 micron and 3.1 micron for the underwater and air stirred welds respectively. These factors, as well as the elevated temperatures the material experiences during FSW, resulted in the evolution of fine equiaxed grains. The overlap region consists of grains of ferrite with very fine particles of dispersed pearlite at the grain boundaries, but there appears to be slightly more pearlite in the air FSW samples compared to the underwater FSW material. However, in all other respects the structures from the two samples were very similar. This is not dissimilar to the structure seen

in the overlap regions of EH46 steel, where the grain size was measured at around 2 micron [21]. This smaller grain size is from a niobium-vanadium microalloyed steel, whereas the carbon steel has no microalloys in it. In addition the EH46 has a smaller overlap region and is significantly thicker (14.5mm).

The microstructure in the middle of the surface showed some differences between the two processes. Typically the air stirred microstructure was more angular and the underwater structure was more predominantly a regular ferrite grain structure. Subjectively, there was more angular ferrite in the air cooled welds than in the underwater weld. However grain size measurements revealed strong similarities for each process. The centre of the weld in the first side was typically 4 microns, and the centre of the weld on the second side was 3 microns.

Overall, the structures of the two welds could be summarized as follows; the underwater weld contained predominantly regular ferrite in the overlap zone and side 2, and in side 1 there was more of a tendency towards an angular ferrite structure ; the air welded samples had a less regular ferrite structure, with a consistent presence of angular ferrite, except in the overlap zone which was regular ferrite.

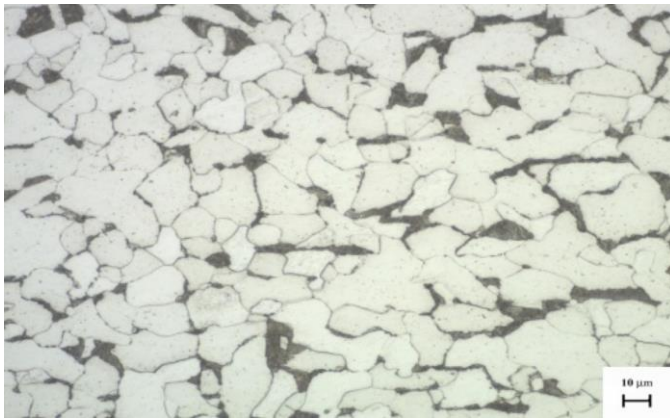


Figure 4 Parent plate material showing ferrite pearlite structure taken at right angles to the major rolling direction, for the air FSW process.

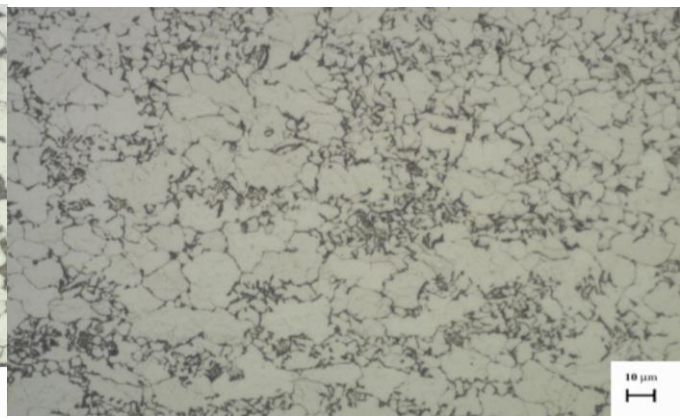


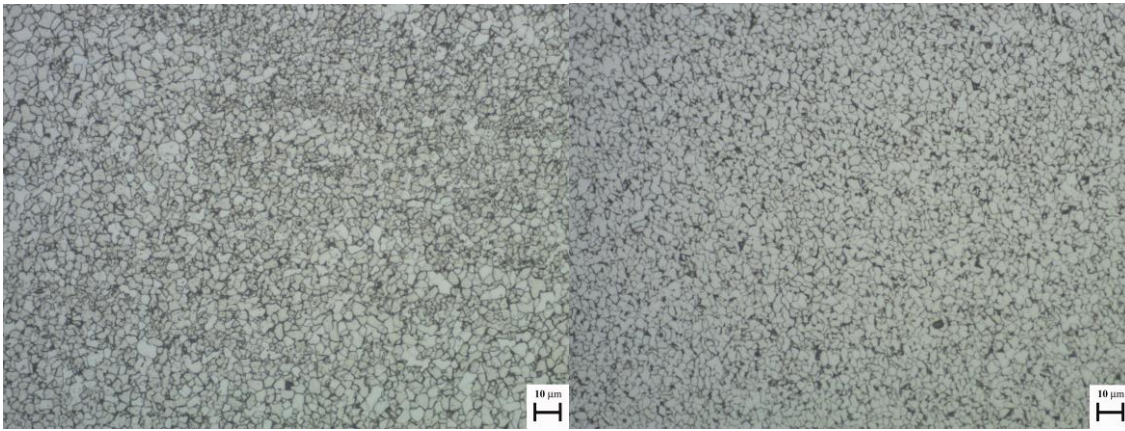
Figure 5(a) TMAZ showing pearlite degeneration in the underwater FSW process



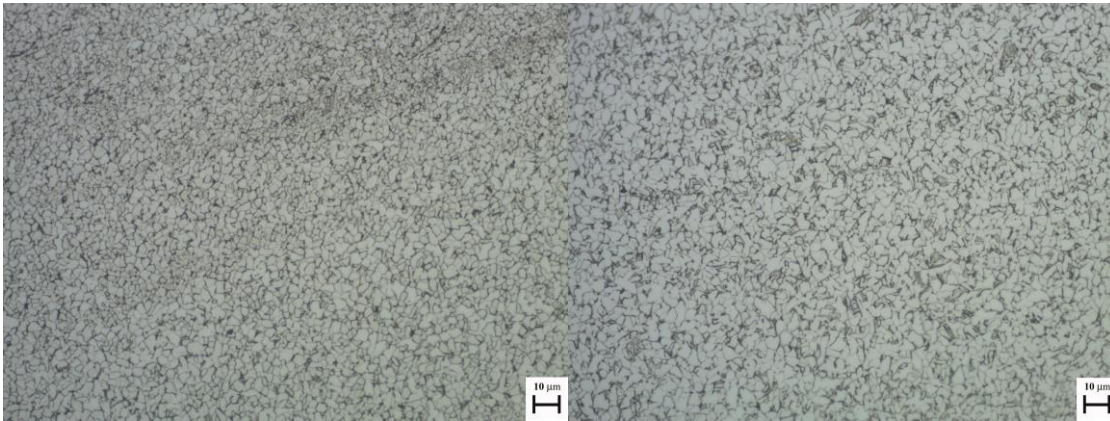
Figure 5(b) TMAZ showing less pearlite degeneration and areas of ferrite recrystallization in the air FSW process.

Underwater

Air



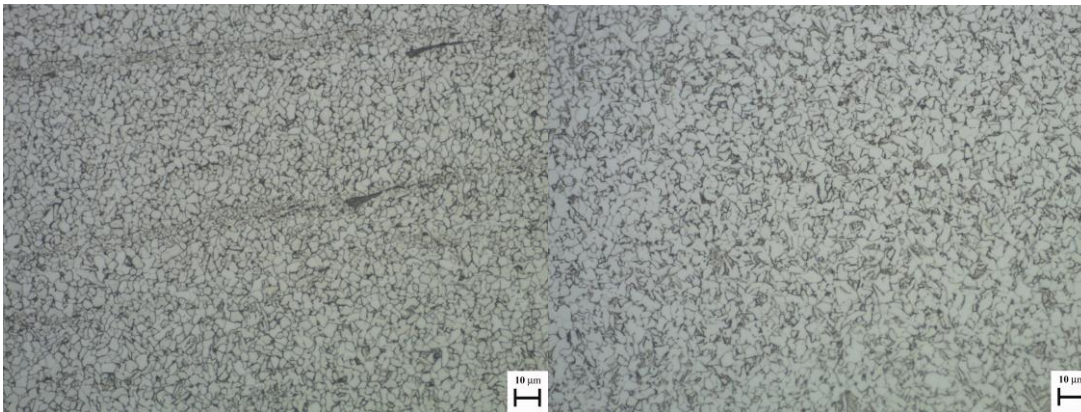
Overlap



Advancing

Side 2

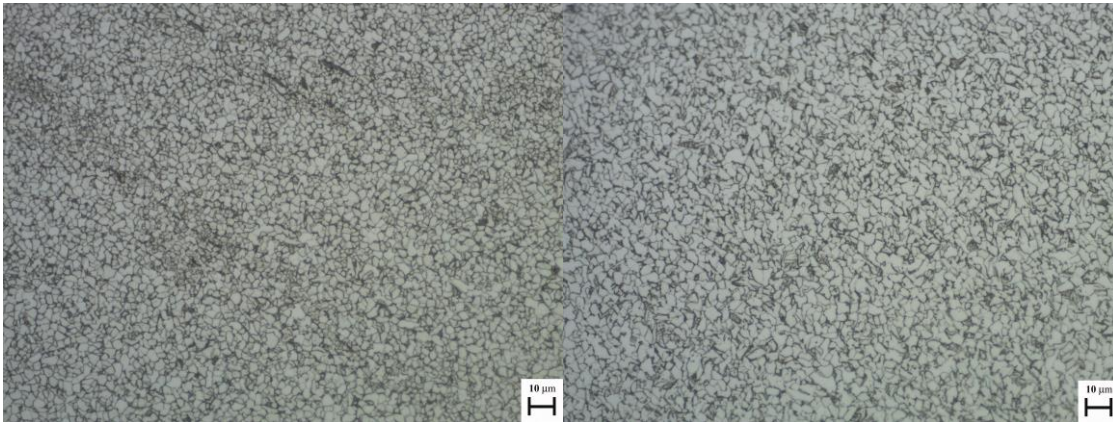
Advancing



Side 2 centre

Underwater

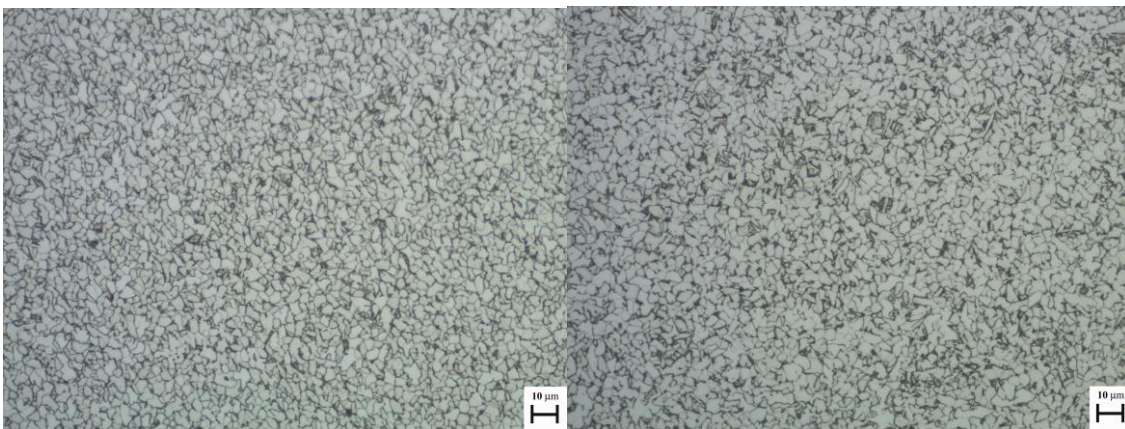
Air



Retreating

Side 2

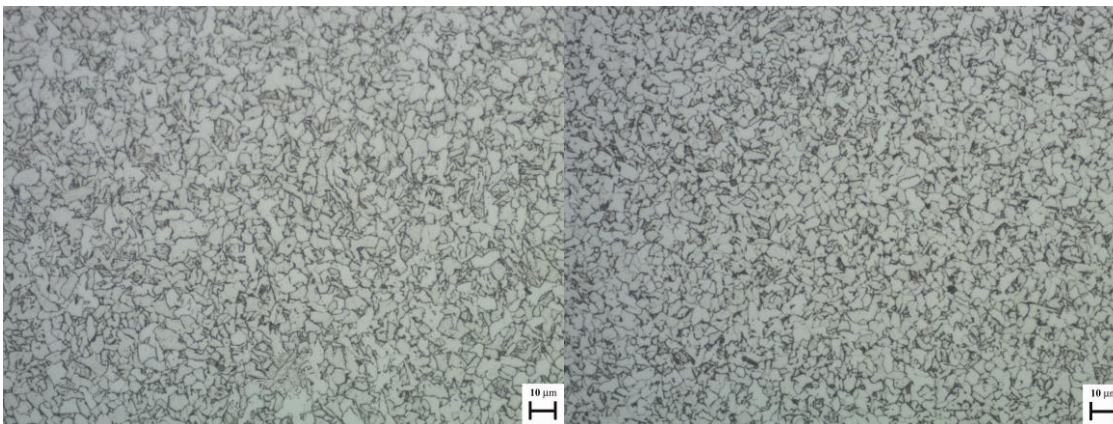
Retreating



Retreating

Side 1

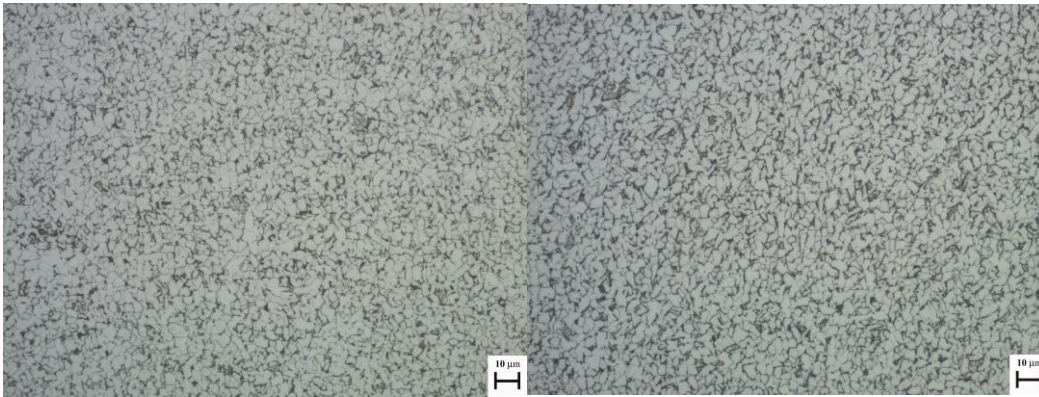
Retreating



Side 1 centre

Underwater

Air



Advancing

Side 1

Advancing

Figure 6 A compilation of the microstructures in specific positions on each sample (underwater on the left and air on the right)

One feature not identified to any significant extent in previous studies of friction stir welded material has been the presence of oxide deposits which appear to have been stirred into the subsurface regions of the weld. This is shown in Figures 7(a) and (b). In some instances the depth of entrainment could reach almost the mid thickness. However this will have been accentuated by the tool design. As stated earlier these plates had received no surface treatment after cutting – so there was oxide and paint primer in the stirring regions. Some of the areas were examined in the Scanning Electron Microscope(SEM) with an EDAX attachment and found to contain no significant levels of silicon or zinc which would normally be indicative of primer. However, in one sample area, shown in Figure 8 only a level of 2.34% silicon was found but the remainder was under 0.50%. It was concluded that it was predominantly surface oxide that had been drawn into the subsurface stirring zones. The remainder of the analysis in that particular point is 23.9% oxygen ; 0.24% chromium ; 0.84% manganese ; 69.9% iron ; 0.43% cobalt ; 0.13% nickel ; 2.17% copper.

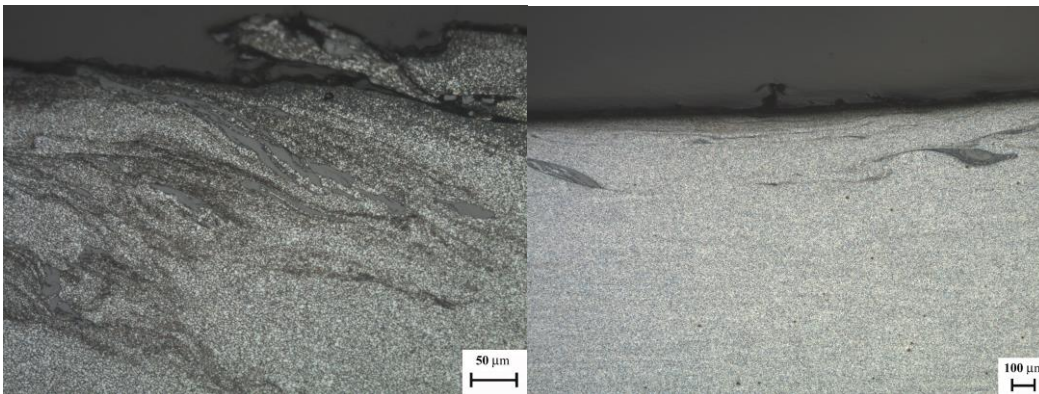


Figure 7 Areas of sub surface showing significant entrainment of scale from the plate surfaces

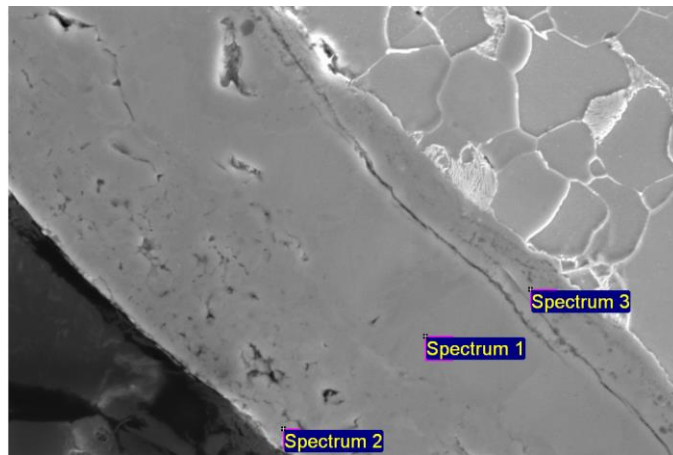


Figure 8 SEM showing oxide area adjacent to steel. Spectrum 3 region had 2.34% silicon from the EDAX analysis

Mechanical Properties

Tensile Strength

In all cases the transverse samples failed in the parent material, highlighting the superior strength of the weld metal. The longitudinal tensile tests produced results with considerably higher mean average yield strength and ultimate tensile strength (UTS) (475 and 577 MPa respectively) than the transverse tensile tests that failed in the parent material (353 and 509 MPa respectively), equating to an improvement of 25.68 and 11.79% for the yield and UTS respectively. There was little difference between the longitudinal tensile strength of the underwater and air welded samples. This enhanced strength within the weld metal was attributed to the microstructure and grain refinement that occurred in the overlap region.

Micro-Hardness

No significant variation in hardness between air and underwater FSW was observed. The micro-hardness did increase in the weld zone by about 26%, but this does not reach a level that would cause any concern at all.

Charpy Impact Toughness

Figure 3(a) shows the relative position of some of the test positions. There can be a significant number of regions contained within one test area, possibly including some small proportion of parent plate. As a result of this there is significant potential to have data with an inherent variability. Changes in the shape of the weld will also influence the toughness due to the relative notch position. The results of the toughness testing at 20, -20 and -40 °C, are shown in Tables 3 and 4. It can be observed that the Charpy impact toughness is significantly reduced for the underwater FSW, attributed ostensibly from a faster cooling rate due to the water environment. However when comparing advancing against retreating side toughness there was no apparent consistency in the results. Other work[19] on DH36 steel has shown a similar inconsistency in toughness data. The explanation probably lies in the finer microstructural mix of the areas that are subjected to the impact test. The variability in toughness of friction stir welded carbon steels may actually be a characteristic of the process, and as data[18] builds up, then a clearer situation will develop. The variation in the microstructure, although on a relatively fine scale in this work could also be indicative of the potential source of the variation in toughness being observed. The work of Guillaume et al [22] showed wide variations in toughness values in the same area and from area to area in 8mm thick DH36 friction stir weld. At -20°C the toughness was lower than that recorded here. However, the microstructure was significantly different to that observed in this work too. In that case it was almost a Widmanstätten structure that was present, which would partially explain the toughness of the weld.

Test Temperature(°C)	Toughness (J)						
	Position						
	Centre line	2mm R	4mm R	6mm R	2mm A	4mm A	6mm A
20	127.5	124.5	81	106.5	144	123	106.5
-20	135	124.5	124.5	93	105	64.5	45
-40	99	115.5	54	37.5	117	135	48
			Retreating side			Advancing side	

Table 3 Charpy toughness (Airweld) in Joules

Test Temperature(°C)	Toughness (J)						
	Position						
	Centre line	2mm R	4mm R	6mm R	2mm A	4mm A	6mm A
20	64.5	102	81	123	87	45	72
-20	82.5	114	114	37.5	63	79.5	130.5
-40	90	64.5	69	19.5	79.5	124.5	126
			Retreating side			Advancing side	

Table 4 Charpy toughness (Underwater weld) in Joules

Fatigue

Low cycle fatigue testing was performed at a stress level of 90% of the measured yield strength. The mean average cycles to failure for the air and underwater specimens being 301K and 745K cycles respectively. Although the ratio of these two mean values may be considerable in absolute terms, there is almost no difference between the longest and shortest lives within each set of results as shown in Tables 5 and 6.

Maximum stress (N/mm ²)	Minimum stress (N/mm ²)	Cycles to failure (K)
311.19	22.93	470
311.91	28.31	312
314.67	31.01	187

Table 5 Low cycle fatigue data for the Air weld

Maximum stress (N/mm ²)	Minimum stress (N/mm ²)	Cycles to failure (K)
314.4	30.84	907
315.49	32.43	469
315.37	31.64	969

Table 6 Low cycle fatigue data for the Underwater weld

To assess the significance of the results, a statistical analysis was performed [23]. The test showed that if the two populations had identical properties there would be a 6.4% probability of obtaining an apparent difference greater than that seen in the experiments. This is marginally higher than the benchmark figure of 5% that would be required before making any claim that the results were significantly different. Comparing the log-normal distributions shown in Fig. 9 (a) it can be seen that there is no significant difference in the fatigue performance of the air and underwater welds. This is further confirmed by considering the pooled data in Fig. 9 (b). If there were two distinct populations (i.e. fatigue life), the graph in Fig. 9 (b) would show some variation from linearity.

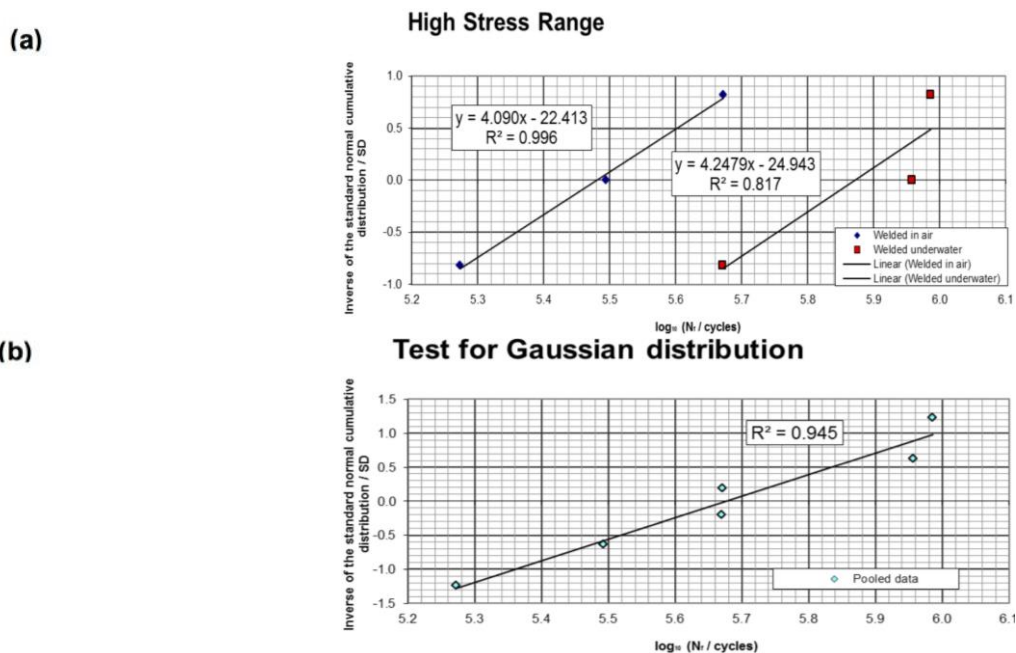


Fig. 9 (a) Log-normal distribution
(b) pooled data, for the air and underwater FSW specimens

CONCLUSIONS

This study has shown that FSW can be successfully completed underwater for S275 structural steel without any adverse effects to the strength, hardness or fatigue life of the material. Charpy impact toughness was however shown to decrease for the underwater weld. Within the available data it is difficult to fully explain the toughness difference as the relative grain sizes do not vary significantly. The potential difference may lie in fine scale differences in the microstructures

Between the processes the longitudinal tensile results are the same, the microhardness does not vary. It was also shown that underwater FSW has benefits compared to SAW and FSW in air. This was apparent in the distortion results where it was shown that FSW underwater significantly reduces angular and longitudinal distortion in the work piece.

Lack of surface preparation can lead to the presence of stirred in oxide particles which can have a localized effect on the grain structure within the welds. This conclusion is made for both FSW conditions in this study.

ACKNOWLEDGMENTS

The authors wish to acknowledge the support of TWI and Tata Steel Europe in this study.

REFERENCES

- [1] W. M. Thomas, K. I. Johnson and C. S. Wiesner, "Friction Stir Welding – Recent Developments in Tool and Process Technologies", *Adv. Eng. Mater.*, 2003, 5, (7), pp. 485-490.
- [2] W. M. Thomas, E. D. Nicholas, J. C. Needham, M. G. Murch, P. Templesmith and C. J. Dawes, "Friction stir welding", International patent application no. PCT/GB92102203 and Great Britain patent application no. 9125978, published 1991.

- [3] M. Posada and S. Roush, "Friction stir welding- a promising new technique for joining metals", *Seaframe*, 2005, 1, (Issue 2), pp. 17-18.
- [4] R. Nandan, T. Debroy and H. K. D. H. Bhadeshia, "Recent advances in friction stir welding- process, weldment structure and properties", *Prog. Mater. Sci.*, 2008, 53, pp. 980-1023.
- [5] A. Simar, Y. Bréchet, B. De Meester, A. Denquin and T. Pardoen, "Microstructure, local and global mechanical properties of friction stir welds in aluminium alloy 6005A-T6", *Mater. Sci. & Eng.*, 2008, A486, pp. 85-95.
- [6] V. Balasubramanian, "Relationship between base metal properties and friction stir welding process parameters", *Mater. Sci. and Eng.*, 2008, A480, pp. 397-403.
- [7] H. K. D. H. Bhadeshia and T. DebRoy, "Critical assessment: friction stir welding of steels", *Sci. and Technol. of Welding and Joining*, 2009, 14, (3), pp. 193-196.
- [8] W. Gan, Z. T. Li and S. Khurana, "Tool materials selection for friction stir welding of L80 steel", *Sci. and Technol. of Welding and Joining*, 2007, 12, pp. 610-613.
- [9] R. Rai, A. De, H. K. D. H. Bhadeshia and T. Debroy, "Review: friction stir welding tools", *Sci. and Technol. of Welding and Joining*, 2011, 16, (4), pp. 325-342.
- [10] J. Perrett, J. Martin, J. Peterson, R. Steel and S. Packer, "Friction Stir welding of industrial steels", TMS annual meeting, 27th February – 3rd March 2011, San Diego, CA, USA.
- [11] C. D. Sorensen, "Evaluation of PCBN pin tool wear during FSW of Structural steel", Friction Stir Sci. and Technol. (ONR), Book of abstracts, PI Review Meeting, York, PA, USA, Oct 2009, pp. 30.
- [12] K. H. Song, H. Fujii and K. Kakata, "Effect of welding speed on microstructural and mechanical properties of friction stir welded Inconel 600", *Mater. and Design*, 2009, 30, pp. 3972-3978.
- [13] H. Fujii, L. Cui, N. Tsuji, M. Maeda, K. Nakata and K. Nogi, "Friction stir welding of carbon steels", *Mater. Sci. and Eng.*, 2006, A 429, pp. 50-57.
- [14] A. K. Lakshminarayanan and V. Balasubramanian, "An assessment of microstructure, hardness, tensile and impact strength of friction stir welded ferritic stainless steel joints", *Mater. and Design.*, December 2010, 31, (Issue 10), pp. 4592-4600.
- [15] H.J. Liu, H.J. Zhang and L. Yu, "Effect of welding speed on microstructures and mechanical properties of underwater friction stir welded 2219 aluminium alloy", *Mater. and Design.*, 2011, 32, pp. 1548-1553.
- [16] W.C. Stewart, "Feasibility of underwater friction stir welding of HY-80 steel", MSc Thesis, Naval Postgraduate School, Monterey, California, 2011.
- [17] T. Gar, P. Mathur, V. Singhal, C. Jain and P. Gupta, "Underwater friction stir welding: An overview", *International Review of Applied Engineering Research*, 2014, 4(2), 165-170.
- [18] A. Toumpis, A.M. Galloway, S.R. Cater and N.A. McPherson, "Development of a process envelope for friction stir welding of DH36 steel – A step change", *Materials and Design*, 2014, 62, 64-75.
- [19] N.A. McPherson, A.M. Galloway, J. Wood and S.R. Cater, "A comparison between friction stir welded and submerged arc welded DH36 steel thin plate", *Trends in Welding Research, Proceedings of the 9th International Conference*, 4-8th June 2012, Chicago, IL, USA.
- [20] T. J. Lienert, W. L. Stellwag, Jr and L. R. Lehman, "Comparison of Heat Inputs: Friction Stir Welding vs. Arc Welding", Edison Welding Institute Columbus, OH 43221.
- [21] T.N. Baker and N.A. McPherson, Unpublished work, University of Strathclyde, 2014.
- [22] G. Rückert, M. Chargy, F. Cortial and F. Jorez, 'Evaluation of FSW on high yield strength steels for shipbuilding' *Materials Science Forum*, 2014, Vols. 783-786, 1776-1781
- [23] *NIST/SEMATECH e-Handbook of Statistical Methods*, <http://www.itl.nist.gov/div898/handbook/>.